Development ePress online publication date 9 July 2008

Development 135, 2739-2746 (2008) doi:10.1242/dev.024059

Dap160/intersectin binds and activates aPKC to regulate cell polarity and cell cycle progression

Chiswili Chabu and Chris Q. Doe*

The atypical protein kinase C (aPKC) is required for cell polarization of many cell types, and is upregulated in several human tumors. Despite its importance in cell polarity and growth control, relatively little is known about how aPKC activity is regulated. Here, we use a biochemical approach to identify Dynamin-associated protein 160 (Dap160; related to mammalian intersectin) as an aPKC-interacting protein in *Drosophila*. We show that Dap160 directly interacts with aPKC, stimulates aPKC activity in vitro and colocalizes with aPKC at the apical cortex of embryonic neuroblasts. In *dap160* mutants, aPKC is delocalized from the neuroblast apical cortex and has reduced activity, based on its inability to displace known target proteins from the basal cortex. Both *dap160* and *aPKC* mutants have fewer proliferating neuroblasts and a prolonged neuroblast cell cycle. We conclude that Dap160 positively regulates aPKC activity and localization to promote neuroblast cell polarity and cell cycle progression.

KEY WORDS: PKC, Cell cycle, Intersectin, Neuroblast, Polarity, Quiescence, *Drosophila*

INTRODUCTION

Asymmetric cell division has been proposed as a mechanism for maintaining stem cell numbers while allowing the generation of differentiated cell types (Morrison and Kimble, 2006). It is also been proposed that asymmetric cell division of a small number of tumor stem cells may be the origin of several tumor types (Morrison and Kimble, 2006). Asymmetric cell division typically involves establishment of a cell polarity axis, followed by alignment of the mitotic spindle with the polarity axis to produce daughter cells with different molecular composition. One evolutionarily conserved protein involved in both cell polarity and asymmetric cell division is atypical protein kinase C (aPKC; called PKC-3 in *C. elegans* and aPKCζ, λ/ι in mammals). aPKC is required for *C. elegans* blastomere cell polarity (Tabuse et al., 1998), *Drosophila* oocyte polarity (Tian and Deng, 2008); *C. elegans*, *Drosophila* and mammalian epithelial polarity (Aranda et al., 2006; Gopalakrishnan et al., 2007; Harris and Peifer, 2007; Helfrich et al., 2007; Hutterer et al., 2004; Nagai-Tamai et al., 2002; Rolls et al., 2003; Suzuki et al., 2004; Suzuki et al., 2002; Takahama et al., 2008; Yamanaka et al., 2006; Yamanaka et al., 2003; Yamanaka et al., 2001); and *Drosophila* planar cell polarity (Djiane et al., 2005); and has been implicated as an oncogene in several human tumors (Fields et al., 2007; Regala et al., 2005; Yi et al., 2008). aPKC is called 'atypical' because unlike classical PKCs or novel PKCs, it is not activated by Ca^{2+} or diacylglycerol, but rather by a relatively poorly understood mechanism of protein-protein interactions.

Drosophila larval brain neural progenitors (neuroblasts) are a powerful system with which to study the role of asymmetric cell division and stem cell self-renewal and proliferation. aPKC is required for both cell polarity and stem cell self-renewal in *Drosophila* neuroblasts (Lee et al., 2006; Rolls et al., 2003). aPKC colocalizes with the polarity proteins Par-6, Cdc42 and Bazooka (Baz; Par3 in mammals) at the apical cortex of mitotic neuroblasts, and is segregated into the self-renewing neuroblast at each cell division. The apical cortical crescent of aPKC ensures exclusion of the differentiation factors Miranda, Prospero, Brain tumor (Brat) and Numb from the apical cortex, resulting in their restriction to the basal cortex and ultimate partitioning into the smaller ganglion mother cell (Doe, 2008; Knoblich, 2008), which typically divides once to form two postmitotic neurons. In *aPKC* mutants neuroblasts, cell polarity is disturbed such that Miranda and Numb basal proteins become distributed uniformly on the neuroblast cell cortex, both at metaphase and at telophase, resulting in a molecularly symmetric cell division and a decrease in neuroblast numbers (Lee et al., 2006; Rolls et al., 2003). aPKC has been proposed to regulate neuroblast cortical polarity by phosphorylating and inhibiting cortical localization of the Lethal giant larvae (Lgl) protein (Betschinger et al., 2003), which is required for basal targeting of Miranda and Numb proteins (Ohshiro et al., 2000; Peng et al., 2000). Overexpression of a membrane-targeted aPKC, but not a kinase dead version, leads to reduced basal protein localization and the formation of supernumerary neuroblasts (Lee et al., 2006), revealing the importance of aPKC kinase activity for promoting neuroblast cell polarity and self-renewal. Despite the central role of aPKC kinase activity in establishing neuroblast cell polarity, relatively little is known about how aPKC activity is regulated. Recently, we showed that the small G-protein Cdc42 is colocalized with aPKC and can stimulate aPKC activity by relieving Par-6 inhibition of aPKC (Atwood et al., 2007). However, the stimulation of activity is modest and the polarity phenotypes of *cdc42* mutant are not fully penetrant, which suggests that additional aPKC activators may exist.

Despite the importance of aPKC in cell polarity and growth control, little is known about how aPKC activity is regulated. Here, we have sought to identify aPKC-interacting proteins using a biochemical approach, and then assay their function in *Drosophila* neuroblasts. We performed immunoprecipitation experiments coupled to mass spectrometry analysis (IP/MS) using aPKC as the bait protein and identified Dap160 (dynamin associated protein-160), a member of the intersectin protein family (Adams et al., 2000). Dap160 was originally identified by its ability to interact with the endocytic protein Dynamin in *Drosophila* head extracts (Roos and Kelly, 1998). *dap160* mutants have nerve terminals with reduced levels of endocytic proteins (Koh et al., 2004; Marie et al., 2004), consistent with a role in endocytosis. However, *dap160* mutants were

Institute of Neuroscience, Institute of Molecular Biology, Howard Hughes Medical Institute, University of Oregon, Eugene, OR 97403, USA.

*Author for correspondence (e-mail: cdoe@uoneuro.uoregon.edu)

Accepted 13 June 2008

also isolated in a genetic screen for modifiers of the Sevenless receptor tyrosine kinase (Roos and Kelly, 1998), showing that Dap160 also regulates signal transduction, similar to mammalian intersectin (Malacombe et al., 2006; Martin et al., 2006; Tong et al., 2000a; Tong et al., 2000b). Here, we show that Dap160 binds aPKC, increases its kinase activity, and that both Dap160 and aPKC are required for neuroblast cell polarity and cell cycle progression.

MATERIALS AND METHODS

Fly stocks and MARCM clones

The wild-type fly stock was *yellow white* (*y w*). The *dap160*^{Q24}, *Df(2)10523*$^{\#35}$ and *UAS-Dap160* stocks were gifts from Graeme Davis (UCSF). *dap160*$^{\Delta 1}$ was a gift from Hugo Bellen (Koh et al., 2004). *aPKC*^{k06643} flies lacking the early embryonic lethal background mutation have been described previously (Rolls et al., 2003). Analysis of cell polarity was carried out in stage 15-16 *dap160*^{Q24}*/Df(2)10523* trans-heterozygotes embryos as previously described (Marie et al., 2004). The hypomorphic *dap160*^{Q24}*/dap160*$^{\Delta 1}$ hetero-allelic combination was used to assay larval brain neuroblast numbers. The *shi*^{ts2} chromosome was a gift from Mani Ramaswami (Arizona). To generate positively marked MARCM clones, we recombined *FRT40* onto the *dap160*^{Q24} chromosome using standard techniques, and used the previously described *FRTG13 aPKC*^{k06403} chromosome (Rolls et al., 2003). *dap160* neuroblast mutant clones were generated by mating *dap160*^{Q24} *FRT40/CyO, actGFP* to *y w hsFLP; FRT40A tubP-GAL80/CyO ActGFP; tubP-GAL4 UAS-mCD8::GFP/TM6 Tb Hu* (Bello et al., 2008). *aPKC*^{k06403} neuroblast mutant clones were generated by mating *FRTG13 aPKC*^{k06403}*/CyO* to *y w hsFLP; FRTG13 tubP-GAL80/CyO actGFP; tubP-GAL4 UAS-mCD8::GFP/TM6 Tb Hu* (C. Cabernard and C.Q.D., unpublished). Clones were induced at 24-28 hours after larval hatching for 1 hour at 37°C and aged for 4 days at 25°C.

In vitro binding assays and immunoprecipitations

GST-tagged Dap160 was engineered by polymerase chain reaction from a P-spaceneedle-Dap160-dsred construct (a gift from Graeme Davis) followed by subcloning into pGEX-4T1 vector (Pharmacia). The construct was verified by DNA sequencing. GST-Dap160 was expressed in BL21 cells overnight at 25°C, adsorbed onto glutathione agarose (Sigma), washed three times with binding buffer [10 mM HEPES (pH 7.5), 100 mM NaCl, 1 mM DTT, 0.1% Tween-20]. We co-incubated GST-Dap160 with Par-6 or aPKC proteins at room temperature for 15 minutes followed by five washes in binding buffer. Interactions were tested by eluting proteins in SDS sample buffer, SDS-PAGE and western blotting. Par-6 and aPKC proteins were a gift from Scott Atwood (Prehoda laboratory, OR). For immunoprecipitation experiments, a 12-hour collection of *y w* embryos was homogenized in lysis buffer [50 mM HEPES (pH 7.5), 150 mM NaCl, 0.1% Tween-20, 1 mM EDTA, 2.5 mM EGTA, 10% glycerol, supplemented with protease inhibitor tablets; Roche] to produce 1 ml of lysate. Lysates were pre-cleared with protein agarose-A beads for 1 hour at 4°C and subsequently divided equally (500 μl each) in two Eppendhorf tubes and incubated with 2 μl of either anti-βgal or anti-aPKC antibodies for 4 hours at 4°C. Lysates were then incubated with protein agarose A beads for 1 hour at room temperature. For pulldowns, beads were precipitated and washed three times in modified lysis buffer containing 1 mM NaCl. Samples were sent to the Fred Hutchinson Cancer Research Center proteomic facility (Seattle, WA) for mass-spectrometry analysis.

Kinase activity assays

aPKC activity assays were carried out as described previously (Atwood et al., 2007). Briefly 0.16 μM aPKC was co-incubated with 50 μM peptide substrate, no Par-6 or 1.14 μM Par-6, no Dap160 or increasing molar concentration of Dap160 protein (0.34, 0.68, 1.02 μM). Phosphorylated peptides were resolved by gel electrophoresis, quantified using ImageJ and normalized to total peptide input.

Antibodies, immunostaining and imaging

An affinity-purified anti-Dap160 antibody was raised against the C-terminal peptide sequence GPF VTS GKP AKA NGT TKK (Alpha Diagnostic). Guinea pig or chicken anti-Dap160 was used at 1:100 (this study); guinea pig or rat anti-Miranda at 1:500 (Doe laboratory); rabbit anti-aPKC at 1:1000 (Sigma), guinea pig anti-Numb at 1:1000 (a gift from Jim Skeath, Missouri); rabbit anti-Scrib at 1:2500 (Doe laboratory); rat monoclonal anti-Dpn (Doe laboratory) at 1:1; mouse anti-Pros monoclonal (purified MR1A at 1:1000; Doe laboratory); rabbit anti-phosphohistone H3at 1:1000 (Sigma, St Louis, MO); rabbit anti-GFP at 1:1000 (Sigma, St Louis, MO); rat anti-Par-6 at 1:250 (Atwood et al., 2007); mouse anti-β galactosidase at 1:500 (Promega); mouse anti-α tubulin (at 1:1500, Sigma); guinea pig anti Sec15 at 1:1500 (Hugo Bellen); rabbit anti-Rab11 at 1-1000 (Donald Ready); and rabbit anti-Dap160 at 1:500 (Marie et al., 2004; Roos and Kelly, 1998). Secondary antibodies were obtained from Molecular Probes (Eugene, OR). Embryos were fixed and stained as described previously (Siegrist and Doe, 2005), except that fixing was carried out in 9% paraformaldehyde for 15 minutes. *shi*^{ts2} embryos were shifted to restrictive temperature (37°C) for 30 minutes and subsequently fixed and stained. Larval brains were dissected, fixed and stained as described previously (Siller et al., 2005), and analyzed with a BioRad Radiance 2000 or Leica TCS SP laser scanning confocal microscope using a 60×1.4 NA oil immersion objective. Images were processed with Illustrator software (Adobe).

For live imaging we used the GFP protein-trap line *G147 (GFP::Jupiter)* that expresses a microtubule-associated GFP fusion protein (Morin et al., 2001), *worniu-GAL4, UAS-GFP::Miranda, UAS-CHERRY::Jupiter* (C. Cabernard and C.Q.D., unpublished) and *worniu-GAL4; UAS-Dap160/TM6B Tb*. Live imaging was performed as previously described (Siller et al., 2005), except that temporal resolution was either 15 seconds for 2-hour imaging intervals or 3 minutes for overnight imaging sessions. The 4D data sets were processed in ImageJ (NIH) and Imaris (Bitplane, Switzerland) software.

Statistical analysis

To test the significance in neuroblast number variation between wild-type, *dap160* mutant and Dap160-overexpressing brains we used a *t*-test (two-tailed distribution and two samples, equal variance). To test the significance in NEBD to AO length variation between wild type, *dap160* and *aPKC* mutants we used a *t*-test (two-tailed distribution and two samples, unequal variance). To test the significance of the differences in polarity protein localization between wild type and *dap160* mutant neuroblasts, we performed a *z*-test using the percent normal crescent for each polarity protein comparing wild type and *dap160* mutants; the difference in percent normal between wild type and *dap160* mutants was significant with a one-tail confidence level greater than 99.6 % for all polarity proteins analyzed.

RESULTS

Dap160 and aPKC are part of the same protein complex

To identify novel components in aPKC pathways of neuroblast cell polarity and neuroblast self-renewal, we sought to identify aPKC/Par-6 interacting proteins by IP/MS using aPKC as our bait protein. IP eluates containing complex mixtures of proteins from a non-specific pull-down (anti-green fluorescent protein; GFP) or anti-aPKC pull down were analyzed by Multiple Dimensions Protein Identification Technology (MUDPIT). These experiments returned Dap160 as a potential aPKC-interacting protein with the highest score of tryptic products hits. Dap160 contains two Eps15 homology domains (EH), a coiled-coil domain (CC) and four Src homology 3 domains (SH3) (Fig. 1A). These domains are conserved in the vertebrate Dap160 homologue intersectin (Fig. 1A), although Dap160 lacks the DH, PH, C2 domains present in the long isoform of intersectin and consequently is not predicted to have GTPase activity (Fig. 1A). Dap160 has two alternative splice variants: a long isoform, which migrates at 160 kDa and a shorter isoform migrating at 120 kDa (Fig. 1A,B).

Next, we sought to verify that Dap160 and aPKC are part of the same protein complex in vivo. An affinity-purified peptide antibody raised against Dap160 C terminus, which recognizes a 160 kDa band

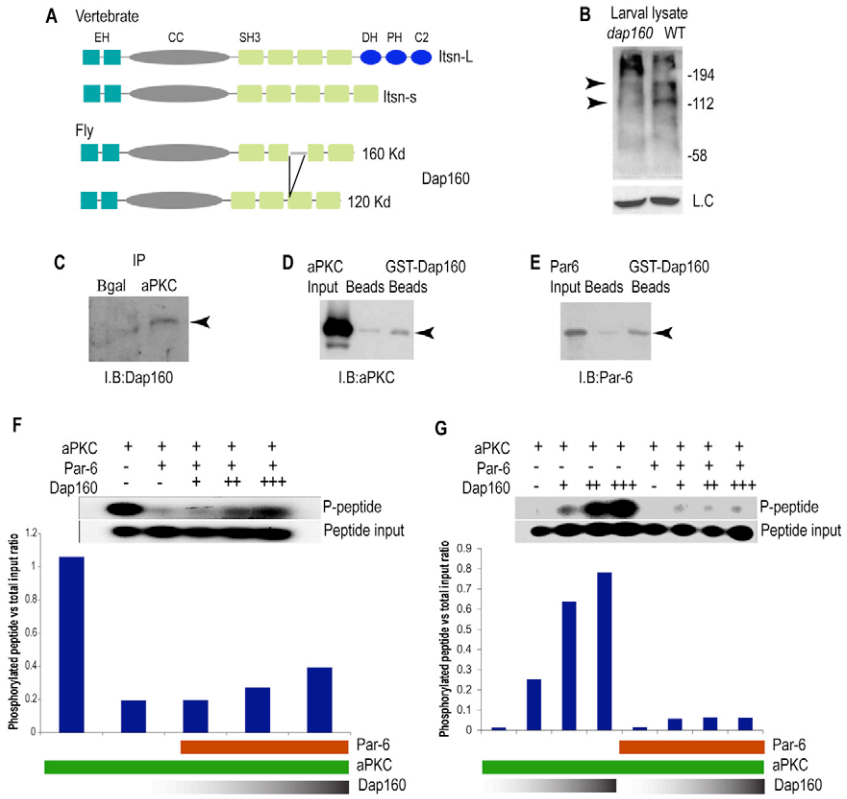

Fig. 1. Dap160 interacts with aPKC. (**A**) *Drosophila* Dap160 and vertebrate intersectin protein domains. (**B**) Dap160 antibody detects two bands in wild-type lysate (top arrow, 160 kDa; bottom arrow, 120 kDa) that may correspond to the two predicted isoforms shown in A; and these bands are absent in lysate from *dap160* mutants, illustrating the specificity of the antibody. An independently generated antibody gives the same result (see Fig. 2N). (**C**) Immunoprecipitation from larval lysate using an aPKC antibody and a control antibody (Bgal) and blotted with a Dap160 antibody shows aPKC co-immunoprecipitates Dap160 protein (arrowhead). (**D**,**E**) In vitro protein interaction experiments. (D) In vitro generated Dap160 protein coupled to glutathione S-transferase (GST) beads can bind in vitro produced aPKC protein (arrowhead). Beads alone do not bind aPKC; input lane shown at left. (E) In vitro generated Dap160 protein coupled to glutathione S-transferase (GST) beads can bind in vitro produced Par-6 protein (arrowhead). Beads alone do not bind Par-6; input lane shown at left. (**F**,**G**) Dap160 directly stimulates aPKC activity and this effect can be partially blocked by Par6. Top: presence (+) or absence (–) of each protein; middle: phosphorylation of the aPKC substrate peptide. Histogram shows quantification of the phosphorylation (bars) over a schematic depiction of protein levels (see Materials and methods for protein concentrations). Note that aPKC alone can have high activity immediately after its synthesis (F) or much lower activity after storage (G), but can still be stimulated by Dap160.

in wild-type larval lysate but not in *dap160* mutant lysate (Fig. 1B), was used to perform aPKC/Dap160 pull-down experiments. We found that Dap160 and aPKC reproducibly co-immunoprecipitate (Fig. 1C), thus indicating that Dap160 and aPKC are present in the same protein complex. We obtained similar results with a second, independently generated Dap160 antibody (Marie et al., 2004; Roos and Kelly, 1998) (Fig. 2M).

Dap160 directly interacts with aPKC to stimulate aPKC activity

We tested whether Dap160-aPKC directly interact using an in vitro protein interaction assay. We incubated full-length N-terminal GST-tagged Dap160 with full-length N-terminal His-tagged aPKC and found that Dap160 can bind aPKC (Fig. 1D). Par-6 and aPKC form a complex in *Drosophila* (Atwood et al., 2007), so we tested for direct interactions between Dap160 and Par-6. We found that full-length Dap160 also directly binds Par-6 (Fig. 1E). We conclude that Dap160 directly interacts with both aPKC and Par-6.

We next tested whether Dap160 increased aPKC activity (similar to the Par-6 binding protein Cdc42) or repressed aPKC activity (similar to the aPKC binding protein Par-6) (Atwood et al., 2007). We co-incubated aPKC protein and a proven fluorescent peptide substrate (Atwood et al., 2007) with increasing amounts of Dap160 protein in the in the presence of Par-6. By measuring the amount of phosphorylated substrate relative to total peptide input, we found that Dap160 increased aPKC activity in a dose-dependent manner (Fig. 1F). To test whether Dap160 stimulation of aPKC is dependent on Par-6, we compared the ability of Dap160 to stimulate aPKC in the presence or absence of Par-6. We found that Dap160 directly stimulates aPKC and that Par-6 could almost completely suppress the ability of Dap160 to activate aPKC (Fig. 1G). Note that aPKC basal activity is variable between experiments (compare Fig. 1F with Fig. 1G) but we found that Dap160 was always able to increase aPKC basal activity. We conclude that the Dap160/aPKC or Dap160/ Par-6/aPKC complex is more active than the aPKC/Par-6 complex.

Dap160 and aPKC co-localize in neuroblasts

To determine whether Dap160 has the potential to activate aPKC in neuroblasts, we examined Dap160 localization during neuroblast asymmetric cell division. In wild-type neuroblasts, Dap160 protein is cytoplasmic at interphase, but becomes enriched at the apical cortex during mitosis (Fig. 2A-D); this is identical to aPKC

localization (Fig. 2G-K) (Rolls et al., 2003). Two different antibodies produced similar staining in wild-type neuroblasts, and showed no apical Dap160 enrichment in *dap160* mutants (Fig. 2B,N), confirming specificity of the antibodies. In larval neuroblasts, Dap160 was undetectable at the cortex at mitosis (Fig. 2E), possibly owing to low protein levels and/or reduced antibody detection sensitivity. Therefore, we used a *UAS-dap160* transgene to overexpress Dap160 in larval neuroblasts, and observed enrichment of Dap160 at the apical cortex (90%, *n*=12; Fig. 2F,L) although weaker ectopic cortical patches could also be observed (66%, *n*=12; Fig. 4K). This provides further support for the specificity of our antibodies for Dap160 protein. We conclude that Dap160 and aPKC are cytoplasmic in interphase neuroblasts, and can be colocalized at the apical cortex of mitotic neuroblasts.

Dap160 promotes aPKC apical localization and kinase activity in neuroblasts

Wild-type mitotic embryonic neuroblasts have apical aPKC, Par-6 and Baz crescents (Fig. 3A-C), and basal Miranda/Numb cortical crescents (Fig. 3D-E). In *dap160* mutant embryonic neuroblasts, aPKC showed ectopic cortical patches beyond the apical cortical domain (71%, *n*=41 neuroblasts from 13 embryos; Fig. 3F); similarly, Par-6 showed ectopic cortical patches beyond the apical cortical domain (50%, *n*=12 from 6 embryos; Fig. 3G). By contrast, Baz was mostly apical but occasionally cytoplasmic (22%, *n*=96 from 35 embryos; Fig. 3H). Cortical aPKC protein may be inactive or less active in *dap160* mutant neuroblasts, because Miranda and Numb proteins showed ectopic cortical localization beyond the basal cortical domain (Miranda, 36%, *n*=55 from 24 embryos; Numb, 38%, *n*=18 from 11 embryos; Fig. 3I,J), similar to a weak *aPKC* mutant phenotype (Rolls et al., 2003). *dap160* mutant neuroblasts never showed cytoplasmic Miranda, but rather we observed that aPKC overlapped with Miranda at the cortex (15%, *n*=13 from five embryos; Fig. 3F,I,J), which is never observed in wild-type neuroblasts (Lee et al., 2006; Rolls et al., 2003). Conversely, Dap160 overexpression in larval neuroblasts results in cortical Dap160 and ectopic cortical patches of aPKC (Fig. 4J,L), as well as depletion of cortical Miranda in some neuroblasts (19%, *n*=21 from 12 larvae; Fig. 4K), suggesting that the ectopic aPKC is at least partially active.

We further investigated Miranda localization by time-lapse analysis of larval neuroblasts expressing GFP::Miranda and the microtubule-binding protein Cherry::Jupiter (C. Cabernard and C.Q.D., unpublished). In wild-type neuroblasts, GFP::Miranda forms basal crescents during mitosis (100%, *n*=37; Fig. 4M). In neuroblasts with overexpression of Dap160, we could observe divisions where Miranda was cytoplasmic (8%, *n*=40 divisions from 19 neuroblasts; Fig. 4N), which we never observed in wild type. We conclude that Dap160 positively regulates aPKC localization and activity, and is required for aPKC-mediated neuroblast cortical polarity.

Dap160 regulates the number of proliferating larval neuroblasts

An important function of aPKC is to maintain larval neuroblast pool size: *aPKC* mutants have fewer proliferating larval brain neuroblasts and overexpression of a membrane-tethered aPKC increases the

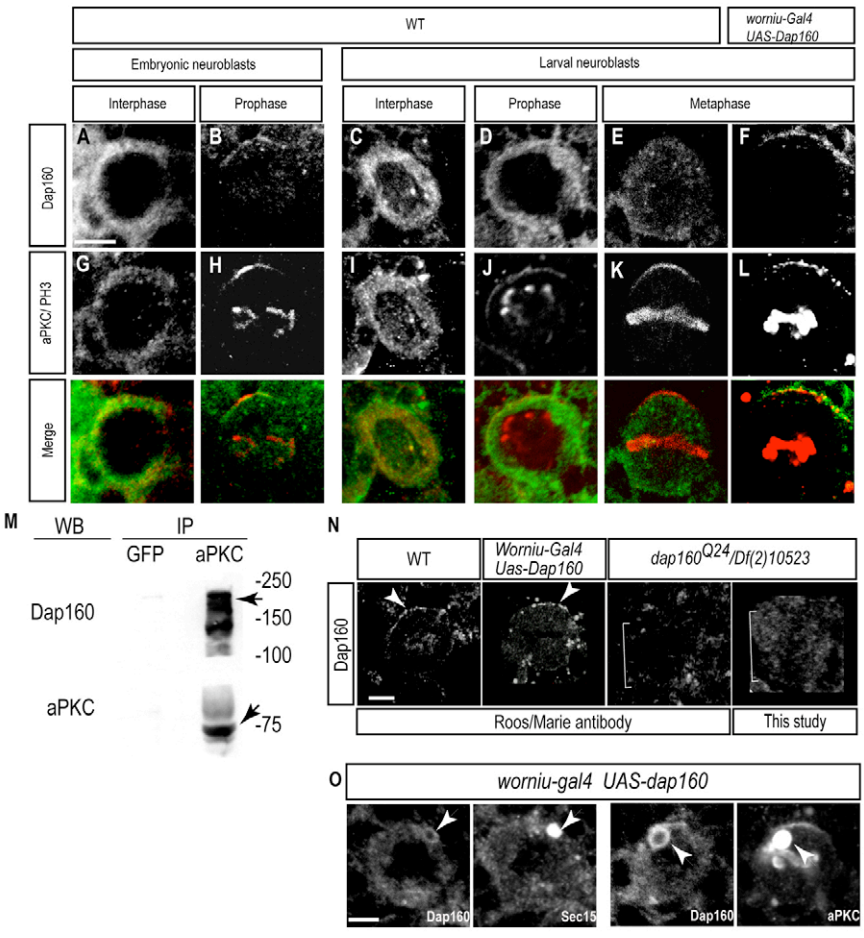

Fig. 2. Dap160 co-localizes with aPKC in neuroblasts. (**A-L**) Neuroblasts co-stained for Dap160 (A-F) and aPKC (G-L); merged images below. Genotypes, developmental stages and cell cycle stages labeled at top. (B,H) Dap160 colocalizes with aPKC at the apical cortex of mitotic embryonic neuroblasts. (E,K) Endogenous Dap160 is undetectable at the site of aPKC apical cortical localization in larval brain metaphase neuroblasts. (F,L) Overexpression of Dap160 reveals colocalization with aPKC at the apical cortex in larval brain metaphase neuroblasts (90%, *n*=12). Scale bar: 5 □m. (**M**) aPKC can immunoprecipitate Dap160 from embryonic lysates. Right lane: aPKC antibody can immunoprecipitate Dap160 (top arrow) and aPKC (bottom arrow). Left lane: the GFP control antibody does not immunoprecipitate either Dap160 or aPKC. (**N**) Two independently generated Dap160 antibodies detect apical crescents of Dap160 in wild-type neuroblasts or Dap160 overexpression neuroblasts (arrowheads) but not in *dap160* mutant neuroblasts (brackets). Roos/Marie antibody from Roos and Kelly (Roos and Kelly, 1998). Scale bar: 5 □m. (**O**) Dap160 overexpression results in the formation of Dap160/Sec15 double-positive puncta in neuroblasts (arrowheads; left pair of panels) and Dap160/aPKC double-positive puncta (arrowheads; right pair of panels). Scale bar: 5 □m.

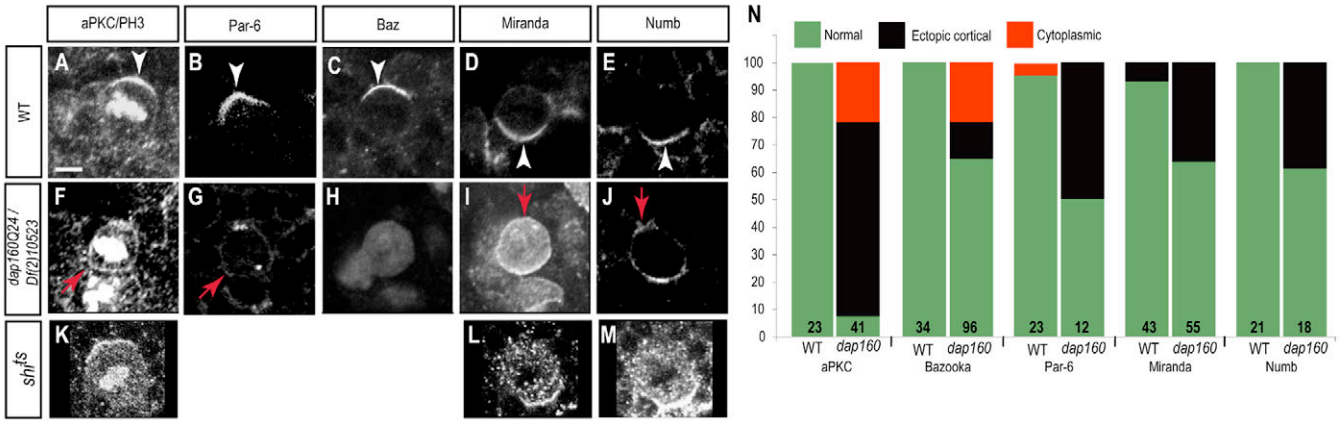

Fig. 3. Dap160 regulates embryonic neuroblast cortical polarity. (**A-E**) Wild type metaphase embryonic stage 15 neuroblasts stained for the indicated proteins (top labels) have apical crescents of aPKC, Bazooka, Par-6 (100%, *n*=23; 100%, *n*=34; and 96%, *n*=23, respectively) and basal crescents of Miranda (93%, *n*=43) and Numb (100%, *n*=21) (white arrowheads). (**F-J**) *dap160* metaphase embryonic stage 15 neuroblasts. (F) aPKC is mostly ectopic cortical aPKC (71%, *n*=41, red arrow) or cytoplasmic (not shown). (G) Par-6 is ectopic cortical (50%, *n*=12, red arrow) or normal (not shown). (H) Baz is cytoplasmic (21.8%, *n*=96; H), ectopic cortical or normal (not shown). (I) Miranda is ectopic cortical (red arrow, 36%, *n*=55) or normal (not shown). (J) Numb is ectopic cortical (red arrow, 38%, *n*=18) or normal (not shown). Proteins are delocalized and may also be at lower levels than in wild-type neuroblasts. (**K-M**) *dynamin* mutant mitotic larval neuroblasts (*shibire*^{ts}/*shibire*^{ts} at restrictive temperature; see Materials and methods) have aPKC apical crescents (K) and basal crescents of Miranda (L) and Numb (M). (**N**) Quantification of the neuroblast cortical polarity phenotypes. Number of neuroblasts scored is shown as a number at the bottom of each bar. Scale bar: 5 μm.

number of larval brain neuroblasts (Lee et al., 2006). Here, we test whether decreasing or increasing Dap160 levels has a similar effect on brain neuroblast numbers. We find that wild-type third larval instar brain lobes contain 96±5 (*n*=5) Deadpan-positive (Dpn$^+$) neuroblasts, whereas similarly staged *dap160* mutants contain only 72.6±6 (*n*=5); *P*=0.0002 Dpn$^+$ neuroblasts (Fig. 4A). We conclude that both Dap160 and aPKC are required to maintain the normal number of proliferating neuroblasts in the larval brain. The loss of neuroblasts in the *dap160* mutant brain could be due to neuroblast death, differentiation or the failure of neuroblasts to exit from quiescence during larval stages (see Discussion).

We next generated *dap160* or *aPKC* mutant single neuroblast clones to determine whether Dap160 (or aPKC) is required within the neuroblast and its progeny for maintaining neuroblast identity.

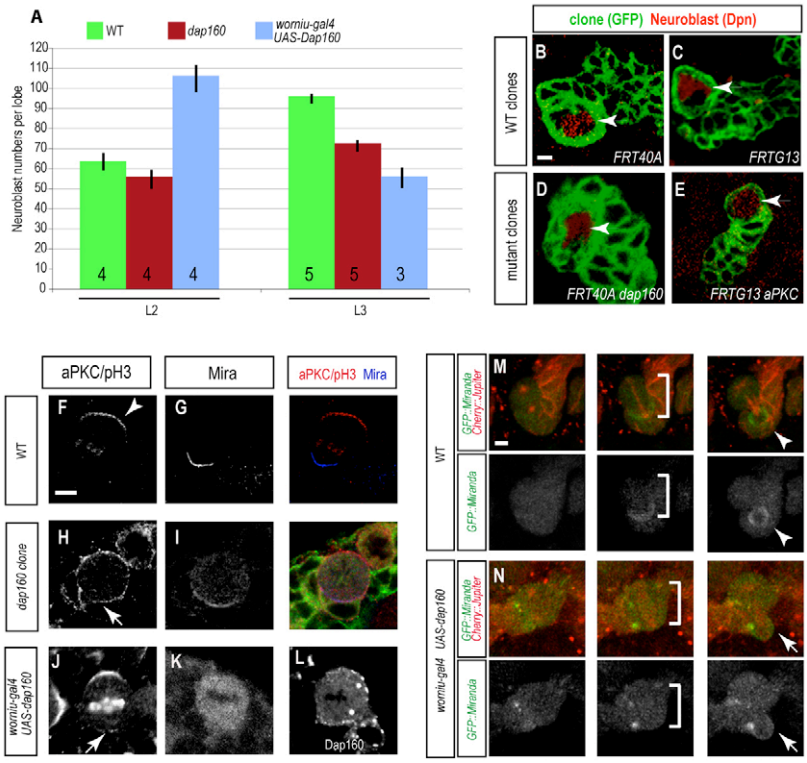

Fig. 4. Dap160 positively regulates neuroblast pool size. (**A**) Neuroblast numbers scored wild-type (green bars), *dap160* mutants (red bars) and Dap160 misexpression larvae at second instar (L2) or wandering third instar (L3). Numbers inside bars indicate numbers of brains analyzed. See Materials and methods for genotypes and growth temperatures. (**B-E**) Wild-type (B,C), *dap160* (D) and *aPKC* (E) mutant clones (*n*⩾50 and *n*=35 respectively) always contain a single Deadpan-positive neuroblast (arrowhead). (**F-L**) Neuroblast cortical polarity in larval neuroblasts. (F,G) Wild-type neuroblasts have aPKC apical crescents (arrowhead) and Miranda (Mira) basal crescents. (H,I) *dap160* mutants have weak ectopic cortical aPKC (arrows) and normal Mira basal crescents (15%, *n*=13). (J,K) Dap160 overexpression in neuroblasts leads to weak ectopic cortical aPKC (arrow), increased cytoplasmic and reduced cortical Mira (19%, *n*=21 as shown; remainder normal basal crescents); Dap160 is detected in cortical patches and cytoplasmic puncta (L). (**M**,**N**) Live imaging of wild-type neuroblasts with GFP::Mira and Cherry::Jupiter. (M) Wild-type neuroblasts show basal GFP::Mira at metaphase (brackets) and partition GFP::Mira to the GMC at telophase (arrowhead; 100%, *n*=37). (N) Dap160 misexpressing neuroblasts show cytoplasmic GFP::Mira at metaphase (brackets) and occasionally do not segregate GFP::Mira to the GMC at telophase (arrow; 8%, *n*=40). Scale bars: 5 μm.

We generated single neuroblast clones in first instar larvae, allowed them to develop for 96 hours and scored them in late third instar larvae (see Materials and methods). Without exception, we found that all *dap160* mutant clones contained a single large Dpn$^+$ neuroblast (n>50 clones in 16 larvae; Fig. 4D). Similarly, all *aPKC* single neuroblast mutant clones retained one Dpn$^+$ neuroblast (n=35 clones in 12 larvae; Fig. 4E). The *dap160* mutant neuroblast clones showed aPKC and Miranda neuroblast polarity phenotypes similar but weaker than observed in *dap160* mutant embryos (compare Fig. 4H,I with Fig. 3). These results may be due to masking of the *dap160* phenotype by residual Dap160 protein in the mutant clone, or due to a role of Dap160 outside the neuroblast lineage in maintaining neuroblast numbers (see Discussion). Nevertheless, we can conclude that Dap160 is required within the neuroblast or its progeny for proper neuroblast cell polarity.

We next determined whether overexpression of Dap160 could affect the number of proliferating neuroblasts. We overexpressed Dap160 using a neuroblast-specific Gal4 driver (*worniu-gal4 UAS-dap160*) and scored the number of Dpn$^+$ larval neuroblasts. We saw no change in the number of larval neuroblasts at first instar (data not shown). At second larval instar, wild-type larvae contain 78±5.6 neuroblasts (n=4; Fig. 4A), whereas larvae overexpressing Dap160 have 106.3±13.9, P=0.03 (n=4; Fig. 4A). This result is consistent with Dap160 inducing ectopic neuroblast self-renewal, similar but much weaker than the increase in neuroblast numbers seen following overexpression of membrane-tethered aPKC (Lee et al., 2006). At third instar, wild-type larvae contain ~96±5 neuroblasts (n=5; Fig. 4A), whereas larvae overexpressing Dap160 have a decline in neuroblast numbers to ~57±10 (n=3; Fig. 4A). This surprising result may be due to neuroblast differentiation, following a graduate accumulation of Miranda/Prospero/Brat differentiation factors in the neuroblasts. This hypothesis is based on our observation that Miranda partitioning into the GMC is defective when assayed in fixed preparations (Fig. 4K) or in live imaging of GFP::Miranda localization (Fig. 4N). Alternatively, prolonged exposure to high Dap160 levels could lead to neuroblast cell death. Taken together, our mutant and misexpression data support a role for both Dap160 and aPKC in maintaining the number of proliferating neuroblasts in the larval brain.

Dap160 and aPKC are required for neuroblast cell cycle progression

We next tested whether Dap160 and aPKC are required for neuroblast cell cycle progression. We performed time lapse imaging of neuroblast cell cycle progression in both *dap160* and *aPKC* mutant larval neuroblasts expressing the spindle marker GFP::Jupiter. Wild-type neuroblasts take 7.76±2.04 (n=15) minutes to transit from nuclear envelope breakdown (NEBD) to anaphase onset (AO; Fig. 5A), consistent with previous reports (Siller et al., 2006; Siller and Doe, 2008; Siller et al., 2005). By contrast, progression through mitosis (NEBD-AO) was delayed in both *dap160* mutants and *aPKC* mutants: 13.37±4.4 minutes, n=10; P=0.006 in *dap160* mutant neuroblasts (Fig. 5B) and 17.84±4.52 minutes, n=11; $P=7.6\times10^{-6}$ in *aPKC* mutant neuroblasts (Fig. 5C). In addition, *dap160* mutant neuroblasts had a longer interphase length (often over 12 hours; data not shown) compared with an average of ~2 hours for wild-type neuroblasts (Siller and Doe, 2008) (C. Cabernard and C.Q.D., unpublished). We conclude that Dap160 and aPKC promote cell cycle progression in larval neuroblasts.

DISCUSSION

aPKC plays an important role in regulating cell polarity, neural stem cell identity and neural stem cell proliferation in vertebrates and invertebrates (Costa et al., 2008; Grifoni et al., 2007; Lee et al., 2006; Rolls et al., 2003). Here, we show that Dap160 positively regulates aPKC activity and localization in neuroblasts, and is required for effective aPKC function in establishing neuroblast cell polarity and cell cycle progression.

Dap160 binds aPKC and increases kinase activity

Par6 directly interacts with aPKC to suppress aPKC activity, while Cdc42 binds Par-6 and modestly upregulates aPKC activity (Atwood et al., 2007; Etienne-Manneville and Hall, 2001; Henrique and Schweisguth, 2003; Hirano et al., 2005). Our study shows that Dap160 directly interacts with both aPKC and Par-6, and can stimulate aPKC activity independent of Par-6. However, Par-6 reduces the ability of Dap160 to stimulate aPKC, suggesting that the Dap160/aPKC complex is more active than Dap160/aPKC/Par6 complex, which in turn is more active than the aPKC/Par6 complex.

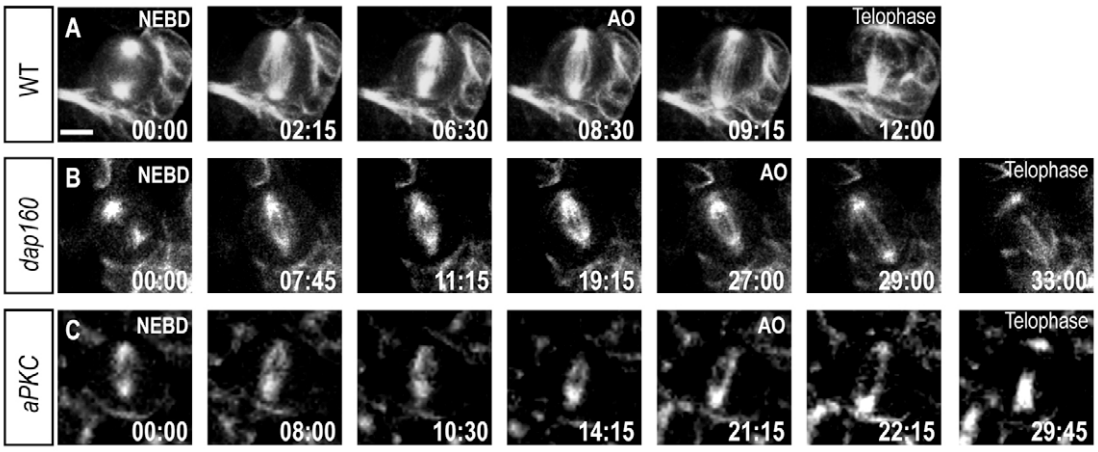

Fig. 5. Dap160 is required for neuroblast cell cycle progression. Wild-type, *dap160* mutant and *aPKC* mutant neuroblasts imaged with Jupiter::GFP from nuclear envelope breakdown (NEBD) to anaphase onset (AO). (**A**) Wild-type neuroblasts have a NEBD-AO interval of 7.76±2.04 minutes; n=15. (**B**) *dap160* mutant neuroblasts have a NEBD-AO interval of 13.37±4.4 minutes; n=10. (**C**) aPKC mutant neuroblasts have a NEBD-AO interval of 17.84±4.52 minutes; n=11. Scale bar: 5 □m.

The exact binding sites for the Dap160/aPKC interaction are unknown; good candidates would be the Dap160 SH3 domains and the two SH3-binding motifs (P-X-X-P) in aPKC.

Dap160 regulates aPKC localization

How does Dap160 promote aPKC localization and activity? Because Dap160 is known to bind Dynamin to regulate endocytosis, it is possible that Dap160 may promote apical aPKC localization by clearing aPKC from the basal cortex. Arguing against this model is our finding that a dynamin mutant (shi^{ts2}) does not affect the apical localization of aPKC or basal localization of Miranda and Numb (Fig. 3K-M; compare with *dap160* phenotype shown in Fig. 3F,I,J). We favor a model in which Dap160 regulates aPKC localization via an endocytosis-independent mechanism. In support of endocytosis-independent functions for Dap160, its vertebrate homolog, intersectin, has both endocytosis and signaling functions. The signaling function requires protein domains shared between Dap160 and intersectin, and includes binding and recruiting mammalian son-of-sevenless (Sos) to the plasma membrane where it regulates Ras signaling (Tong et al., 2000a; Tong et al., 2000b).

Dap160 may promote aPKC localization indirectly, by increasing aPKC kinase activity. aPKC is required to stabilize the Par complex (Baz/Par-3, Par-6, aPKC) in many cell types, including neuroblasts (Atwood et al., 2007), and it is likely that lowered aPKC activity would destabilize anchoring proteins such as Bazooka from the neuroblast apical cortex. In support of this model, we observe a weakening of the Bazooka crescent in *dap160* mutant embryonic neuroblasts.

Another possibility is that Dap160 regulates aPKC cortical polarity via vesicle transport. Consistent with this model, Dap160 controls synaptic vesicle transport in *Drosophila* nerve terminals (Marie et al., 2004), and aPKC (PKC-3), Par-6 and Cdc42 regulate vesicle transport in *C. elegans* embryos and mammalian cells (Balklava et al., 2007). In fact, Dap160 overexpression in neuroblasts results in enlarged vesicles that are positive for aPKC and the exocyst marker Sec15 (Fig. 2O and data not shown), suggesting that Dap160 may direct aPKC-positive vesicles to the apical cortex. One appealing model that awaits testing is that polarized vesicle transport localizes Par proteins to the neuroblast apical cortex, and in turn Par proteins restrict differentiation factors such as Miranda and Numb to the basal cortex.

dap160 mutant embryonic neuroblasts have defects in Baz localization, but *dap160* mutant larval neuroblasts show normal Baz localization (data not shown). This may reflect a difference in the mechanism of Baz localization between embryonic and larval neuroblasts, because *aPKC* mutants also have normal Baz localization in larval neuroblasts (Rolls et al., 2003).

Dap160 and aPKC promote neuroblast cell cycle progression

We provide the first evidence that Dap160 and aPKC promote cell cycle progression in neuroblasts. The related vertebrate aPKCζ regulates cell proliferation in *Xenopus* oocytes, mouse fibroblasts and in human glioblastoma cell lines (Berra et al., 1993; Donson et al., 2000), indicating that aPKC promotes cell cycle progression in many cell types. Similarly, the vertebrate Dap160-related intersectin protein is sufficient to induce oncogenic transformation of rodent fibroblasts (Adams et al., 2000), indicating that intersectin can also promote cell cycle progression. It would be interesting to investigate the relationship between intersectin and PKCζ in this tumor model system.

Dap160 and aPKC maintain proliferating neuroblast pool size

We find that both *dap160* and *aPKC* mutant larvae have a partial reduction in the number of proliferating neuroblasts (this work; Lee et al., 2006b). This may be due to neuroblasts differentiating or dying. We cannot exclude neuroblast death, although we see no difference in caspase 3 staining (a cell death marker) between wild-type and mutant larval brains (data not shown). Differentiation of the mutant neuroblasts is more likely, based on our observation that the Miranda differentiation factor scaffolding protein frequently fails to be properly segregated into the GMC during neuroblast asymmetric cell division in *dap160* or *aPKC* mutants. Arguing against this model is the fact that *dap160* or *aPKC* single neuroblast mutant clones maintain a single neuroblast in all cases examined. It is possible that the mutant single neuroblast clones may not fully deplete Dap160 or aPKC protein, e.g. owing to a long half-life of the mRNA or protein. Indeed, neuroblasts in *dap160* mutant clones have a weaker cortical polarity phenotype than neuroblasts in *dap160* organismal mutants, consistent with the presence of residual Dap160 protein in the clones. Alternatively, loss of Dap160 or aPKC outside of the neuroblast lineage may lead to the observed decrease in neuroblast numbers in the whole animal mutants, and this would not be seen in the single neuroblast mutant clones.

Misexpression of Dap160 produces a modest increase in the number of proliferating neuroblasts in second instar larvae, whereas misexpression of cortically tethered aPKC results in a dramatic expansion of neuroblast numbers at all larval stages (Lee et al., 2006). It is likely that activity levels of aPKC are limiting in Dap160 overexpression experiments: unknown proteins(s) may oppose Dap160 stimulation of aPKC (similar to Par-6) leading to a weakly active aPKC and thus causing only a modest increase in neuroblast numbers. Surprisingly, we found that prolonged misexpression of Dap160, into the third larval instar, resulted in loss of neuroblasts. This could be due to neuroblast cell death caused by continued exposure of the neuroblast to elevated levels of Dap160 protein.

We thank Graeme Davis, Bruno Marie, Hugo Bellen, Scott Atwood, Donald Ready and Mani Ramaswami for providing reagents. We thank Laurina Manning for technical assistance. We also thank members of the Doe laboratory, Bruce Bowerman and Kenneth Prehoda for comments on the manuscript. This work was supported by HHMI and AHA pre-doctoral fellowship (0615592Z).

References

Adams, A., Thorn, J. M., Yamabhai, M., Kay, B. K. and O'Bryan, J. P. (2000). Intersectin, an adaptor protein involved in clathrin-mediated endocytosis, activates mitogenic signaling pathways. *J. Biol. Chem.* **275**, 27414-27420.

Aranda, V., Haire, T., Nolan, M. E., Calarco, J. P., Rosenberg, A. Z., Fawcett, J. P., Pawson, T. and Muthuswamy, S. K. (2006). Par6-aPKC uncouples ErbB2 induced disruption of polarized epithelial organization from proliferation control. *Nat. Cell Biol.* **8**, 1235-1245.

Atwood, S. X., Chabu, C., Penkert, R. R., Doe, C. Q. and Prehoda, K. E. (2007). Cdc42 acts downstream of Bazooka to regulate neuroblast polarity through Par-6 aPKC. *J. Cell Sci.* **120**, 3200-3206.

Balklava, Z., Pant, S., Fares, H. and Grant, B. D. (2007). Genome-wide analysis identifies a general requirement for polarity proteins in endocytic traffic. *Nat. Cell Biol.* **9**, 1066-1073.

Bello, B. C., Izergina, N., Caussinus, E. and Reichert, H. (2008). Amplification of neural stem cell proliferation by intermediate progenitor cells in Drosophila brain development. *Neural Develop.* **3**, 5.

Berra, E., Diaz-Meco, M. T., Dominguez, I., Municio, M. M., Sanz, L., Lozano, J., Chapkin, R. S. and Moscat, J. (1993). Protein kinase C zeta isoform is critical for mitogenic signal transduction. *Cell* **74**, 555-563.

Betschinger, J., Mechtler, K. and Knoblich, J. A. (2003). The Par complex directs asymmetric cell division by phosphorylating the cytoskeletal protein Lgl. *Nature* **422**, 326-330.

Costa, M. R., Wen, G., Lepier, A., Schroeder, T. and Gotz, M. (2008). Par-complex proteins promote proliferative progenitor divisions in the developing mouse cerebral cortex. *Development* **135**, 11-22.

Djiane, A., Yogev, S. and Mlodzik, M. (2005). The apical determinants aPKC and dPatj regulate Frizzled-dependent planar cell polarity in the Drosophila eye. *Cell* **121**, 621-631.
Doe, C. Q. (2008). Neural stem cells: balancing self-renewal with differentiation. *Development* **135**, 1575-1587.
Donson, A. M., Banerjee, A., Gamboni-Robertson, F., Fleitz, J. M. and Foreman, N. K. (2000). Protein kinase C zeta isoform is critical for proliferation in human glioblastoma cell lines. *J. Neurooncol.* **47**, 109-115.
Etienne-Manneville, S. and Hall, A. (2001). Integrin-mediated activation of Cdc42 controls cell polarity in migrating astrocytes through PKCzeta. *Cell* **106**, 489-498.
Fields, A. P., Frederick, L. A. and Regala, R. P. (2007). Targeting the oncogenic protein kinase Ciota signalling pathway for the treatment of cancer. *Biochem. Soc. Trans.* **35**, 996-1000.
Gopalakrishnan, S., Hallett, M. A., Atkinson, S. J. and Marrs, J. A. (2007). aPKC-PAR complex dysfunction and tight junction disassembly in renal epithelial cells during ATP depletion. *Am. J. Physiol. Cell Physiol.* **292**, C1094-C1102.
Grifoni, D., Garoia, F., Bellosta, P., Parisi, F., De Biase, D., Collina, G., Strand, D., Cavicchi, S. and Pession, A. (2007). aPKCzeta cortical loading is associated with Lgl cytoplasmic release and tumor growth in Drosophila and human epithelia. *Oncogene* **26**, 5960-5965.
Harris, T. J. and Peifer, M. (2007). aPKC controls microtubule organization to balance adherens junction symmetry and planar polarity during development. *Dev. Cell* **12**, 727-738.
Helfrich, I., Schmitz, A., Zigrino, P., Michels, C., Haase, I., le, Bivic, A., Leitges, M. and Niessen, C. M. (2007). Role of aPKC isoforms and their binding partners Par3 and Par6 in epidermal barrier formation. *J. Invest. Dermatol.* **127**, 782-791.
Henrique, D. and Schweisguth, F. (2003). Cell polarity: the ups and downs of the Par6/aPKC complex. *Curr. Opin. Genet. Dev.* **13**, 341-350.
Hirano, Y., Yoshinaga, S., Takeya, R., Suzuki, N. N., Horiuchi, M., Kohjima, M., Sumimoto, H. and Inagaki, F. (2005). Structure of a cell polarity regulator, a complex between atypical PKC and Par6 PB1 domains. *J. Biol. Chem.* **280**, 9653-9661.
Hutterer, A., Betschinger, J., Petronczki, M. and Knoblich, J. A. (2004). Sequential roles of Cdc42, Par-6, aPKC, and Lgl in the establishment of epithelial polarity during Drosophila embryogenesis. *Dev. Cell* **6**, 845-854.
Knoblich, J. A. (2008). Mechanisms of asymmetric stem cell division. *Cell* **132**, 583-597.
Koh, T. W., Verstreken, P. and Bellen, H. J. (2004). Dap160/intersectin acts as a stabilizing scaffold required for synaptic development and vesicle endocytosis. *Neuron* **43**, 193-205.
Lee, C. Y., Robinson, K. J. and Doe, C. Q. (2006). Lgl, Pins and aPKC regulate neuroblast self-renewal versus differentiation. *Nature* **439**, 594-598.
Malacombe, M., Ceridono, M., Calco, V., Chasserot-Golaz, S., McPherson, P. S., Bader, M. F. and Gasman, S. (2006). Intersectin-1L nucleotide exchange factor regulates secretory granule exocytosis by activating Cdc42. *EMBO J.* **25**, 3494-3503.
Marie, B., Sweeney, S. T., Poskanzer, K. E., Roos, J., Kelly, R. B. and Davis, G. W. (2004). Dap160/intersectin scaffolds the periactive zone to achieve high-fidelity endocytosis and normal synaptic growth. *Neuron* **43**, 207-219.
Martin, N. P., Mohney, R. P., Dunn, S., Das, M., Scappini, E. and O'Bryan, J. P. (2006). Intersectin regulates epidermal growth factor receptor endocytosis, ubiquitylation, and signaling. *Mol. Pharmacol.* **70**, 1643-1653.
Morin, X., Daneman, R., Zavortink, M. and Chia, W. (2001). A protein trap strategy to detect GFP-tagged proteins expressed from their endogenous loci in Drosophila. *Proc. Natl. Acad. Sci. USA* **98**, 15050-15055.
Morrison, S. J. and Kimble, J. (2006). Asymmetric and symmetric stem-cell divisions in development and cancer. *Nature* **441**, 1068-1074.
Nagai-Tamai, Y., Mizuno, K., Hirose, T., Suzuki, A. and Ohno, S. (2002). Regulated protein-protein interaction between aPKC and PAR-3 plays an essential role in the polarization of epithelial cells. *Genes Cells* **7**, 1161-1171.
Ohshiro, T., Yagami, T., Zhang, C. and Matsuzaki, F. (2000). Role of cortical tumour-suppressor proteins in asymmetric division of Drosophila neuroblast. *Nature* **408**, 593-596.
Peng, C. Y., Manning, L., Albertson, R. and Doe, C. Q. (2000). The tumour-suppressor genes lgl and dlg regulate basal protein targeting in Drosophila neuroblasts. *Nature* **408**, 596-600.
Regala, R. P., Weems, C., Jamieson, L., Khoor, A., Edell, E. S., Lohse, C. M. and Fields, A. P. (2005). Atypical protein kinase C iota is an oncogene in human non-small cell lung cancer. *Cancer Res.* **65**, 8905-8911.
Rolls, M. M., Albertson, R., Shih, H. P., Lee, C. Y. and Doe, C. Q. (2003). Drosophila aPKC regulates cell polarity and cell proliferation in neuroblasts and epithelia. *J. Cell Biol.* **163**, 1089-1098.
Roos, J. and Kelly, R. B. (1998). Dap160, a neural-specific Eps15 homology and multiple SH3 domain-containing protein that interacts with Drosophila dynamin. *J. Biol. Chem.* **273**, 19108-19119.
Siegrist, S. E. and Doe, C. Q. (2005). Microtubule-induced Pins/Galphai cortical polarity in Drosophila neuroblasts. *Cell* **123**, 1323-1335.
Siller, K. H. and Doe, C. Q. (2008). Lis1/dynactin regulates metaphase spindle orientation in Drosophila neuroblasts. *Dev. Biol.* (in press).
Siller, K. H., Serr, M., Steward, R., Hays, T. S. and Doe, C. Q. (2005). Live imaging of Drosophila brain neuroblasts reveals a role for Lis1/dynactin in spindle assembly and mitotic checkpoint control. *Mol. Biol. Cell* **16**, 5127-5140.
Siller, K. H., Cabernard, C. and Doe, C. Q. (2006). The NuMA-related Mud protein binds Pins and regulates spindle orientation in Drosophila neuroblasts. *Nat. Cell Biol.* **8**, 594-600.
Suzuki, A., Ishiyama, C., Hashiba, K., Shimizu, M., Ebnet, K. and Ohno, S. (2002). aPKC kinase activity is required for the asymmetric differentiation of the premature junctional complex during epithelial cell polarization. *J. Cell Sci.* **115**, 3565-3573.
Suzuki, A., Hirata, M., Kamimura, K., Maniwa, R., Yamanaka, T., Mizuno, K., Kishikawa, M., Hirose, H., Amano, Y., Izumi, N. et al. (2004). aPKC acts upstream of PAR-1b in both the establishment and maintenance of mammalian epithelial polarity. *Curr. Biol.* **14**, 1425-1435.
Tabuse, Y., Izumi, Y., Piano, F., Kemphues, K. J., Miwa, J. and Ohno, S. (1998). Atypical protein kinase C cooperates with PAR-3 to establish embryonic polarity in Caenorhabditis elegans. *Development* **125**, 3607-3614.
Takahama, S., Hirose, T. and Ohno, S. (2008). aPKC restricts the basolateral determinant PtdIns(3,4,5)P3 to the basal region. *Biochem. Biophys. Res. Commun.* **368**, 249-255.
Tian, A. G. and Deng, W. M. (2008). Lgl and its phosphorylation by aPKC regulate oocyte polarity formation in Drosophila. *Development* **135**, 463-471.
Tong, X. K., Hussain, N. K., Adams, A. G., O'Bryan, J. P. and McPherson, P. S. (2000a). Intersectin can regulate the Ras/MAP kinase pathway independent of its role in endocytosis. *J. Biol. Chem.* **275**, 29894-29899.
Tong, X. K., Hussain, N. K., de Heuvel, E., Kurakin, A., Abi-Jaoude, E., Quinn, C. C., Olson, M. F., Marais, R., Baranes, D., Kay, B. K. et al. (2000b). The endocytic protein intersectin is a major binding partner for the Ras exchange factor mSos1 in rat brain. *EMBO J.* **19**, 1263-1271.
Yamanaka, T., Horikoshi, Y., Suzuki, A., Sugiyama, Y., Kitamura, K., Maniwa, R., Nagai, Y., Yamashita, A., Hirose, T., Ishikawa, H. et al. (2001). PAR-6 regulates aPKC activity in a novel way and mediates cell-cell contact-induced formation of the epithelial junctional complex. *Genes Cells* **6**, 721-731.
Yamanaka, T., Horikoshi, Y., Sugiyama, Y., Ishiyama, C., Suzuki, A., Hirose, T., Iwamatsu, A., Shinohara, A. and Ohno, S. (2003). Mammalian Lgl forms a protein complex with PAR-6 and aPKC independently of PAR-3 to regulate epithelial cell polarity. *Curr. Biol.* **13**, 734-743.
Yamanaka, T., Horikoshi, Y., Izumi, N., Suzuki, A., Mizuno, K. and Ohno, S. (2006). Lgl mediates apical domain disassembly by suppressing the PAR-3-aPKC-PAR-6 complex to orient apical membrane polarity. *J. Cell Sci.* **119**, 2107-2118.
Yi, P., Feng, Q., Amazit, L., Lonard, D. M., Tsai, S. Y., Tsai, M. J. and O'Malley, B. W. (2008). Atypical protein kinase C regulates dual pathways for degradation of the oncogenic coactivator SRC-3/AIB1. *Mol. Cell* **29**, 465-476.